PHOTONIC SENSORS / Vol. 8, No. 4, 2018: 303–309

Detection of Ethanol Using a Tunable Interband Cascade Laser at 3.345μm

Hui GAO[1,2], Liang XIE[1,2*], Ping GONG[1], and Hui WANG[1]

[1]*State Key Laboratory on Integrated Optoelectronics, Institute of Semiconductors, Chinese Academy of Sciences, Beijing 100083, China*

[2]*College of Materials Science and Opto-Electronics Technology, University of Chinese Academy of Sciences, Beijing 101407, China*

[*]Corresponding author: Liang XIE E-mail: xiel@semi.ac.cn

Abstract: With the progress of the laser manufacturing technology, trace gas sensors based on tunable interband cascade lasers (ICLs) and quantum cascade lasers (QCLs) have been widely used to detect organic compounds with high sensitivity. Compared with overtone and combination bands in the near infrared region, for many species, the intensities of fundamental rotational-vibrational absorption bands in the mid-infrared region are much stronger. In this paper, we demonstrate an ethanol sensor using a room-temperature continuous-wave (CW) tunable ICL laser as a light source to detect ethanol vapor concentration with high sensitivity. Combined with the first harmonic (1f) normalized second harmonic (2f) wavelength modulation spectroscopy (WMS) technology, the characteristics of the harmonics of the system are analyzed, and the amplitude of the first harmonic decrease with an increased concentration of ethanol has been demonstrated both theoretically and experimentally. As a result, a detection limitation of 28 ppb is achieved.

Keywords: Ethanol sensor; interband cascade lasers; wavelength modulation spectroscopy

Citation: Hui GAO, Liang XIE, Ping GONG, and Hui WANG, "Detection of Ethanol Using a Tunable Interband Cascade Laser at 3.345 μm," *Photonic Sensors*, 2018, 8(4): 303–309.

1. Introduction

The measurements of ethanol play an important role in the food and microbiological industries, clinical studies, forensic science, and environmental analyses [1]. A varieties of methods and strategies for the determination of this analyte have been reported for different purposes. Quantitative detection of ethanol is traditionally dominated by laboratory analytical technologies such as chromatography, spectrometry, and refractometry [2, 3]. But these conventional analytical methods often require relatively expensive instruments which are laborious, complex, and time-consuming to operate. Electrochemical- and bio-sensors with the small size and low cost perform well in detecting ethanol at a low concentration level, however they suffer from limited lifetimes and cross-response issues. Some detection methods based on optical absorption spectroscopy, such as differential absorption lidar (DIAL) [4, 5], Fourier transform infrared spectroscopy (FTIR) [6–8], and wavelength modulation spectroscopy-tunable diode laser absorption spectroscopy (WMS-TDLAS) [9–11],

Received: 4 December 2017 / Revised: 30 May 2018

DOI: 10.1007/s13320-018-0471-3
Article type: Regular

have also been developed for the efficient detection of ethanol. The DIAL systems make use of the well-known physical phenomenon of "difference absorption" using two laser beams at different wavelengths. They can analyze the sample without the necessity to collect it and are full automation of the measurement, while requiring precise and complex optical systems which are expensive. FTIR measurements have active and passive modes. The active mode uses a controlled, high-temperature infrared source, and the passive experiment uses a naturally occurring infrared radiance as the light source. The systems can be used to detect many kinds of analytes but suffer the disadvantages of bulkiness, complexity, and uncontrolled background source radiance variability.

WMS-TDLAS has advantages of fast response, noninvasion, and non-contact, minimal drift, and high gas specificity. And it has proven to be an excellent tool for sensitive detection in environment because of the use of the correlation detection technology [12]. Owing to its prominent performance, it has been applied in a wide range of applications, such as disease monitoring and diagnostics by breath analysis, commercial production process control, safety supervision in petrochemical industries, and environmental protection [13–16]. The light source is one of the most important components in a trace gas sensing system based on WMS. Due to the lack of suitable tunable light source in the mid-infrared region, WMS is mainly used to detect species with strong absorption feature in the near-infrared region in the past few decades. In recent years, quantum cascaded lasers (QCLs) [17] with a spectral range of 3.7 μm –12 μm and interband cascaded lasers (ICLs) [18] with a spectral range of 2.6 μm – 6 μm provide advantages in terms of continuous-wave (CW), distributed feedback (DFB), high output power levels, and compactness, which make them extremely suitable for a high sensitivity optical trace gas sensor [19, 20]. For many species, especially complex molecular compounds such as propane (C_3H_8), propene (C_3H_6), and ethanol (C_2H_6O), the fundamental rotational-vibrational transitions in the mid-infrared region are several orders of magnitude more intense than transitions in the overtone and combination bands in the near-infrared region [21, 22]. Therefore, the developments of ICL and QCL based WMS gas sensor can permit higher detection sensitivity for more interesting species.

In this paper, we develop an optical sensor to detect the concentration of ethanol at the normal pressure and room temperature. To improve precision and sensitivity of detection, a compact and CW ICL at 3.345 μm close to the strong absorption peak of ethanol is employed. The widely used WMS technology and 1f-normalized-2f technology are applied in this sensor.

2. Basic theory

The fundamental theory, giving the relationship between the incident intensity and transmitted intensity of the light beam after interacting with a uniform medium, is the well-known Beer-Lambert law as

$$I_t = I_0(t)\exp[-P \cdot S(T) \cdot C \cdot L \cdot g(\nu)] \quad (1)$$

where P is the total gas pressure, $S(T)$ is the line strength at a certain temperature, L is the length over which light and gas interact, C is the mole fraction of the absorbing gas, and $g(\nu)$ is the absorption profile at frequency ν [23]. In WMS measurement, the wavelength of laser is modulated by a ramp current and a higher frequency sine wave [24], which can be expressed as

$$\nu = \nu_0 + a \cdot \cos(wt) \quad (2)$$

where ν_0 is the central wavelength of laser, and a is the maximum modulation depth. The intensity of laser is simultaneously modulated, and the instantaneous laser intensity $I_0(t)$ is determined by

$$I_0(t) = \overline{I_0}[1 + i_1 \cos(wt + \varphi_1) + i_2 \sin(2wt + \varphi_2)] \quad (3)$$

where $I_0(t)$ is the modulated output intensity, $\overline{I_0}$ is the average laser intensity over the modulation

period, i_1 is the linear modulation coefficient with a phase shift φ_1, and i_2 is the nonlinear modulation coefficients with a phase shift φ_2. The shift phases φ_1 and φ_2 occur between the laser intensity and reference sinusoidal frequency. Substituting (2) and (3) into (1) and expanding the formula with Fourier cosine series for harmonics detection, the signals of the first harmonic (1f) and second harmonic (2f) at the line center of absorption feature can be written as

$$S_{1f-re}(\nu_0)=\frac{G\overline{I_0}}{2}\left[C_1+i_1\left(C_0+\frac{C_2}{2}\right)\cos(\varphi_1)+\frac{i_2}{2}(C_1+C_3)\cos(\varphi_2)\right]\cos(wt) \quad (4)$$

$$S_{1f-im}(\nu_0)=\frac{G\overline{I_0}}{2}\left[i_1\left(\frac{C_2}{2}-C_0\right)\sin(\varphi_1)+\frac{i_2}{2}(C_3-C_1)\sin(\varphi_2)\right]\sin(wt) \quad (5)$$

$$S_{2f-re}(\nu_0)=\frac{G\overline{I_0}}{2}\left[C_2+\frac{i_1}{2}(C_1+C_3)\cos(\varphi_1)+i_2\left(C_0+\frac{C_4}{2}\right)\cos(\varphi_2)\right]\cos(2wt) \quad (6)$$

$$S_{2f-im}(\nu_0)=\frac{G\overline{I_0}}{2}\left[\frac{i_1}{2}(C_3-C_1)\sin(\varphi_1)+i_2\left(\frac{C_4}{2}-C_0\right)\sin(\varphi_2)\right]\sin(2wt) \quad (7)$$

where G accounts for the optical-electrical gain of the detection system and the later transmission losses due to scattering, beam steering, and window fouling. The Fourier series coefficients C_k are defined as

$$C_0=\frac{1}{2\pi}\int_{-\pi}^{\pi}\exp(-\alpha(\nu)\cdot C\cdot L)d(wt) \quad (8)$$

$$C_k=\frac{1}{\pi}\int_{-\pi}^{\pi}\exp(-\alpha(\nu)\cdot C\cdot L)\cdot\cos(kwt)d(wt) \quad (9)$$

where $\alpha(\nu)=P\cdot S(T)\cdot g(\nu)$. It is a positive symmetric even function at the central wavelength of the absorption peak, which means C_0 is much larger than other Fourier series coefficients when the light absorption is very small. When there is no target gas in the light path, the background amplitudes of 2f and 1f can be written as follows:

$$S_{2f}(\nu_0)=\frac{G\overline{I_0}}{2}i_2 \quad (10)$$

$$S_{1f}(\nu_0)=\frac{G\overline{I_0}}{2}i_1. \quad (11)$$

The nonlinear effect of laser results in the nonzero amplitude of 2f even though there is no absorbance in the light path, but the phase of 2f can be used to distinguish the background noise of 2f introduced by laser. According to the expression of 1f signal, the nonlinear factors i_2 and φ_2 have impact on the amplitude of 1f, but the influence factor on the 1f is quite small under the low light absorbance condition. Moreover, the phase of 1f does not change. Therefore, the equations of 2f and 1f used in the system are modified as

$$S_{2f}(\nu_0)=\sqrt{[S_{2f-re}(\nu_0)]^2+[S_{2f-im}(\nu_0)]^2}\cdot\sin(\theta+\varphi) \quad (12)$$

$$S_{1f}(\nu_0)=\sqrt{[S_{1f-re}(\nu_0)]^2+[S_{1f-im}(\nu_0)]^2} \quad (13)$$

where θ is the phase of 2f, and φ is the compensation phase that can be set in program. θ is the phase difference between the sinusoidal modulation signal and the detector received signal, which mainly results from the time delay between the power modulation and wavelength modulation of laser by the modulated injection current. In order to improve the signal to noise ratio at the central wavelength of the absorption peak, the value of $\sin(\theta+\varphi)$ should equal to one. The value of θ can be directly read from the lock-in amplifiers. Therefore, the compensation phase φ is $\pi/2-\theta$.

Figure 1 shows the absorption spectra of ethanol based on Pacific Northwest National Laboratory (PNNL) database. The data show two narrow features at 3345 nm (2989 cm^{-1}) and 3447 nm (2900 cm^{-1}) with a half width around 0.55 nm and 2.3 nm respectively on a broader absorption feature. It is obvious that the absorption peak at 3345 nm (2989 cm^{-1}) is narrower, and the absorption intensity is stronger. The peak absorbance (base-10) is close to 3×10^{-4} for a gas concentration of 1 ppm × meter,

which makes this feature suitable for the high sensitivity detection of ethanol. Due to the nonzero absorption on both sides of the narrow sharp absorption peak, the amplitude of the first harmonic also changes with the concentration of ethanol.

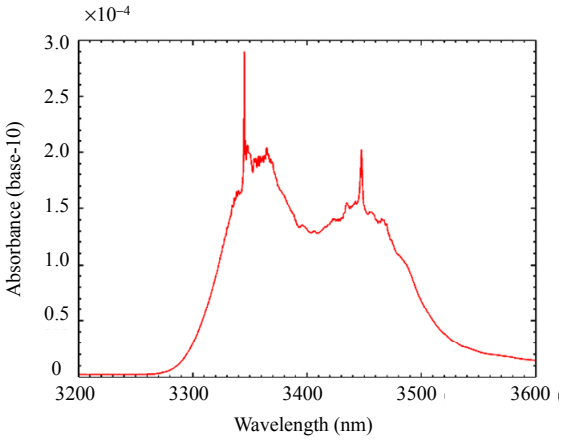

Fig. 1 Spectra of ethanol from 3200 nm to 3600 nm.

3. Experimental setup and results

The schematic diagram of the ethanol sensor architecture is depicted in Fig. 2(a), which includes both the optical and electrical parts. In the optical part, an ICL laser (Nanoplus S/N: 1740/1-30), feature CW, temperature control (TEC), and distribute feedback (DFB), with TO66 package is employed as the excitation source. In order to collimate the laser beam, a coated aspherical lens (Thorlabs modelC036TME) is used. Then, an isolator (Thorlabs Model IO-4-3400-WG) is applied to eliminate the influence of reflection light, which is harmful to the stability of laser. The gas cell is self-made with two protected gold mirrors (Thorlabs CM508-200EH4-M02) for Herriott Cells and two CaF_2 windows (Thorlabs Model WG50530) to ensure air tightness and offers a 10.5 m effective optical path length with a 690 mL sampling volume and 29 reflection times on two mirrors. To simplify the optical alignment of the reported sensor architecture, a dichroic mirror (d=25.4 mm) is used to combine a red alignment laser beam with the mid-infrared ICL beam to track the ICL beam. The light beam, output from the gas cell after interacting with the target ethanol gas, is then focused onto the detector (VIGO SYSTEM S.A model PVI-2TE-3.4) through a 40 mm focal length CaF_2 lens (Thorlabs model LA5370). The detector that is mounted in a TO8 header is made of variable gap HgCdTe semiconductor, and the active area is 1 mm × 1 mm. All the optical devices are assembled on an optical platform as shown in Fig. 2(b).

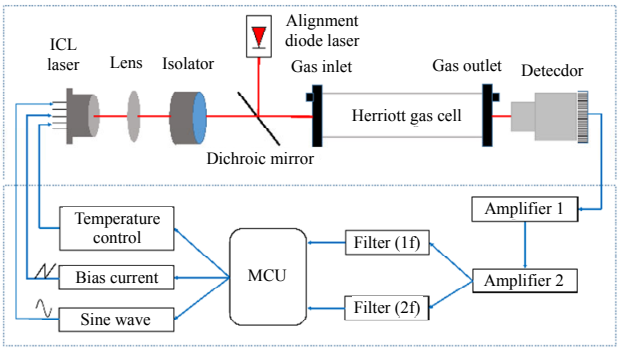

(a)

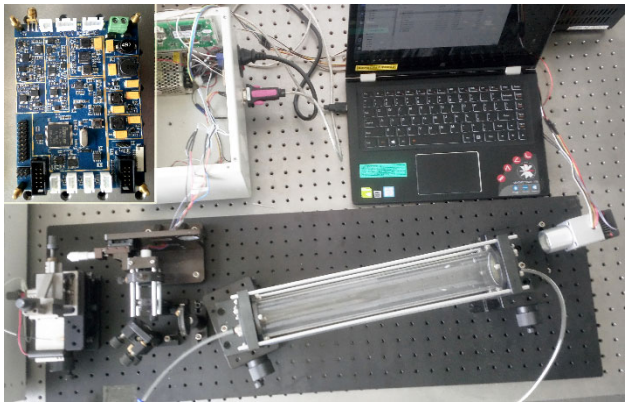

(b)

Fig. 2 Architecture of ethanol sensor: (a) experimental schematic of the ethanol sensor and (b) photo of the sensor platform and integrated circuit plate.

The electrical element of the sensor system is based on a laboratory autonomous developed circuit, which integrates some necessary modules displayed in Fig. 2(a) in a traditional TDLAS system, and some critical parameters can be modified through debug tools. The current of laser is modulated by the triangular wave and sinusoidal wave simultaneously, and ICL temperature is controlled by a professional temperature control chip with a temperature stability to 0.001 centigrade to ensure reliable output

wavelength of laser emitting radiation close to the ethanol absorption peak. The current signal from the detector is transformed into voltage by circuit and amplified with a high precision, low distortion, and low noise complementary metal oxide semiconductor transistor (CMOS) amplifier and then filtered on two channels with a central frequency corresponding to the frequency of the first harmonic and second harmonic, respectively. The 1f and 2f are sampled with two different analog digital conversion (ADC) channels of microcontroller unit (MCU) and then operated by the program with the lock-in amplify (LIA) algorithm.

The ICL has a wavelength of 3345 nm in order to target the ethanol absorption peak at 2989.6 cm^{-1}. It can be operated at temperatures between 15 ℃ and 25 ℃ with a driving current from 28 mA to 75 mA. The measured *P-I* (power-current) curves are shown in Fig. 3(a). The emission wavenumbers in different temperatures and driving currents are depicted in Fig. 3(b). In the ethanol sensing system, the laser temperature is set to 24 ℃, and the driving current scans periodically from 53 mA to 63 mA to target the desired ethanol absorption peak. The sinusoidal modulation signal imposed on the laser has a frequency of 5 kHz, and the amplitude is set to 4.12 mA to get a better signal-noise-ratio (SNR). The sampling rate of AD is 160 kHz for both channels. As a result, each 1f period contains 32 data points, and each 2f period contains 16 data points.

In the experiment, a gas dilution system (Sabio, model 2010) is employed to get samples with different concentrations. We demonstrate that this ethanol sensor can be used to detect ethanol with a high sensitivity. A series of ethanol samples with the concentration from 0 ppm to 3 ppm have been detected and are continuously measured over a period of 5 minutes. Then, the measuring data at different concentration levels are pieced together, and the results are shown in Fig. 4. The value of max 2f increases as the concentrations increase, and the data are negative due to the nonlinear of *P-I* curve of

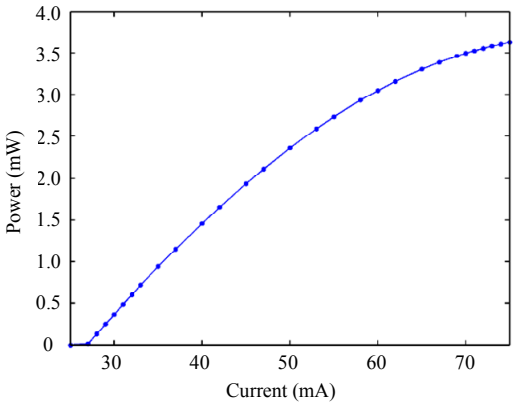

(a)

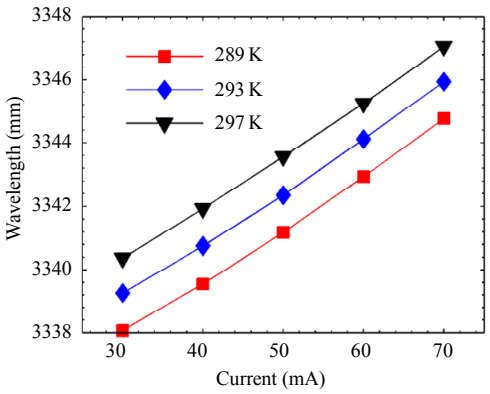

(b)

Fig. 3 Features of ICL laser: (a) measured *P-I* curve for ICL laser operating at 293 K and (b) emission wavelength of laser for different temperatures and driving currents.

ICL. However, this phenomenon has no effect on the measurement results since the background signal caused by ICL can be removed with calibration. In Fig. 4(b), the value of mean 1f decreases as the concentration levels increase, which results from the broader absorption on the both sides of narrow sharp absorption peak. To eliminate the influence of ICL power variations and transmission losses due to scattering, beam steering and window fouling, self-calibration 2f/1f technology and fitting algorithms are used. In Fig. 5, a linear relationship is observed between the max(2f) and mean(1f), and C is given as follows:

$$C = 51.5296x + 8.6709 .$$

In addition, we also assess the detection limit with noise equivalent concentration. A 28 ppb detection limit has been obtained. The response time

of our ethanol sensor is less than 0.6 s.

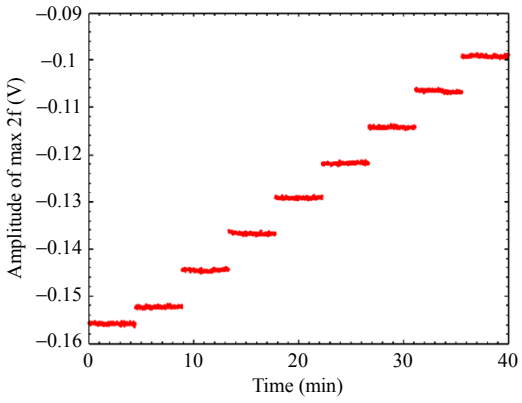

(a)

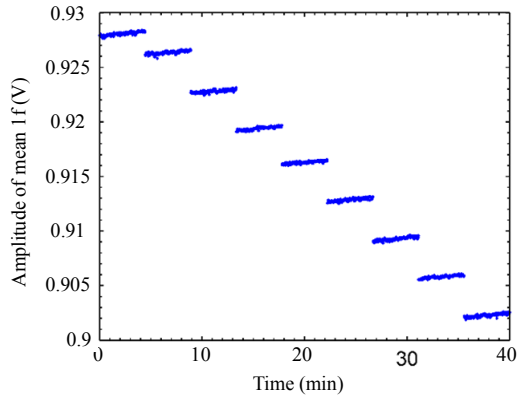

(b)

Fig. 4 Measured second and first harmonics versus different concentrations: (a) amplitude of max second harmonic (2f) and (b) amplitude of mean first harmonic (1f) versus measurement time for 0 ppm, 0.2 ppm, 0.6 ppm, 1 ppm, 1.4 ppm, 1.8 ppm, 2.2 ppm, 2.6 ppm, and 3 ppm ethanol concentration levels.

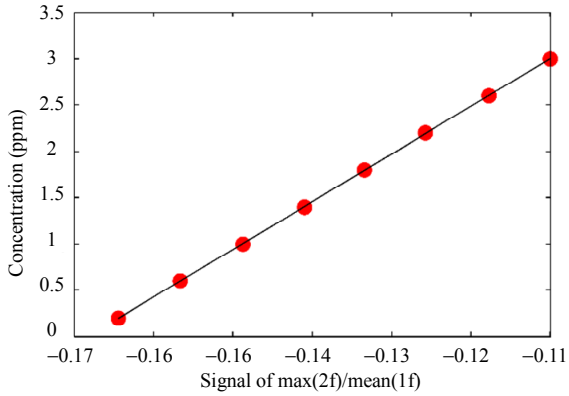

Fig. 5 Actual concentration points and fitting curves of concentration levels versus max(2f)/mean(1f).

4. Conclusions

In this paper, we report the design and performance of an ethanol sensor based on a compact, CW, TEC, and DFB ICL. The ICL with a wavelength of 3345 nm combined with 2f/1f-WMS is applied to a narrow sharp absorption peak located at around 3345 nm (2989.6 cm^{-1}) in order to achieve ethanol measurements at ppb level concentration levels. We obtain a minimum detectable concentration of 28 ppb, and the system response time is less than 0.6 s. The integrated circuit with an advanced RISC (reduced instruction-set computer) machine microprocessor-based controller developed by laboratory aiming at trace gas sensor based on the WMS technology makes it suitable for portable applications. The performance achieved shows that the sensor with the high sensitivity and short response time can be applied in application of disease monitoring, breath analysis, aided diagnosis, and so on. A future sensor upgrade will improve the design of optical components to suppress optical fringes and further optimize the efficiency of the program to remotely detect the concentration of ethanol in moving cars.

Acknowledgment

This work was supported by the State Commission of Science Technology of China (Grant No. 2017YFB0405304).

References

[1] Y. V. Rodionov, O. I. Keppen, and M. V. Sukhacheva, "A photometric assay for ethanol," *Applied Biochemistry and Microbiology*, 2002, 38(4): 395–396.

[2] Y. S. Chen and J. H. Huang, "Arrayed CNT-Ni nanocomposites grown directly on Si substrate for amperometric detection of ethanol," *Biosens Bioelectron*, 2010, 26(1): 207–212.

[3] L. V. Shkotova, A. P. Soldatkin, M. V. Gonchar, W.

Schuhmann, and S. V. Dzyadevych, "Amperometric biosensor for ethanol detection based on alcohol oxidase immobilised within electrochemically deposited Resydrol film," *Materials Science & Engineering C-Biomimetic and Supramolecular Systems*, 2006, 26(2–3): 411–414.

[4] M. Schuetz, J. Bufton, and C. R. Prasad, "A mid-IR DIAL system using interband cascade laser diodes," in *Proceeding of Conference on Lasers and Electro-Optics/Quantum Electronics and Laser Science Conference and Photonic Applications Systems Technologies*, Baltimore, Maryland, USA, 2007, pp. 1–2.

[5] J. Kubicki, J. Mlynczak, and K. Kopczynski, "Application of modified difference absorption method to stand-off detection of alcohol in simulated car cabins," *Journal of Applied Remote Sensing*, 2013, 7(8): 1–13.

[6] P. O. Idwasi, G. W. Small, R. J. Combs, R. B. Knapp, and R. T. Kroutil, "Multiple filtering strategy for the automated detection of ethanol by passive Fourier transform infrared spectrometry," *Applied Spectroscopy*, 2001, 55(11): 1544–1552.

[7] T. Tarumi, G. W. Small, R. J. Combs, and R. T. Kroutil, "Remote detection of heated ethanol plumes by airborne passive Fourier transform infrared spectrometry," *Applied Spectroscopy*, 2003, 57(11): 1432–1441.

[8] J. M. Garrigues, A. Perez-Ponce, S. Garrigues, and M. D. L. Guardia, "Direct determination of ethanol and methanol in liquid samples by means of vapor phase-Fourier transform infrared spectrometry," *Vibrational Spectroscopy*, 1997, 15(2): 219–228.

[9] A. Nadezhdinskii, A. Berezin, Y. Bugoslavsky, O. Ershov, and V. Kutnyak, "Application of near-IR diode lasers for measurement of ethanol vapor," *Spectrochimica Acta Part a-Molecular and Biomolecular Spectroscopy*, 1999, 55(10): 2049–2055.

[10] S. Jie, Q. J. Tang, C. Cheng, and Z. Y. Li, "Remote detection of alcohol concentration in vehicle based on TDLAS," in *Proceeding of Symposium on Photonics & Optoelectronic*, Chengdu, China, 2010, pp. 1–3.

[11] H. Geng, J. G. Liu, Y. J. Zhang, R. F. Kan, Z. Y. Xu, L. Yao, *et al.*, "Ethanol vapor measurement based on tunable diode laser absorption spectroscopy," *Acta Physica Sinica*, 2014, 63(4): 114–119.

[12] J. Hodgkinson and R. P. Tatam, "Optical gas sensing: a review," *Measurement Science and Technology*, 2103, 24(1): 012004-1–012004-95.

[13] C. J. Wang and P. Sahay, "Breath analysis using laser spectroscopic techniques: breath biomarkers, spectral fingerprints, and detection limits," *Sensors*, 2009, 9(10): 8230–8262.

[14] P. Kluczynski, S. Lundqvist, S. Belahsene, Y. Rouillard, L. Nähle, M. Fischer, *et al.*, "Detection of propane using tunable diode laser spectroscopy at 3.37 μm," *Applied Physics B*, 2012, 108(1): 183–188.

[15] L. F. Zhang, F. Wang, L. B. Yu, J. H. Yan, and K. F. Cen, "The research for trace ammonia escape monitoring system based on tunable diode laser absorption spectroscopy," *Spectroscopy and Spectral Analysis*, 2015, 35(6): 1639–1642.

[16] A. K. Andersson, J. Kron, M. Castren, A. M. Athlin, B. Hok, and L. Wiklund, "Assessment of the breath alcohol concentration in emergency care patients with different level of consciousness," *Scandinavian Journal of Trauma Resuscitation & Emergency Medicine*, 2015, 23(1): 1–9.

[17] F. Capasso, "High-performance midinfrared quantum cascade lasers," *Optical Engineering*, 2010, 49(11): 111102-1–111102-9.

[18] I. Vurgaftman, M. Kim, C. S. Kim, W. W. Bewley, C. L. Canedy, J. R. Lindle, *et al.*, "Challenges for mid-IR interband cascade lasers," *Novel in-Plane Semiconductor Lasers Ix*, 2010, 7616(1): 82–88.

[19] C. G. Li, L. Dong, C. T. Zheng, and F. K. Tittel, "Compact TDLAS based optical sensor for ppb-level ethane detection by use of a 3.34 μm room-temperature CW interband cascade laser," *Sensors and Actuators B-Chemical*, 2016, 232: 188–194.

[20] L. Dong, F. K. Tittel, C. G. Li, N. P. Sanchez, H. P. Wu, C. T. Zheng, *et al.*, "Compact TDLAS based sensor design using interband cascade lasers for mid-IR trace gas sensing," *Optics Express*, 2016, 24(6): 528–535.

[21] J. Jagerska, B. Tuzson, H. Looser, A. Bismuto, J. Faist, H. Prinz, *et al.*, "Highly sensitive and fast detection of propane-butane using a 3 μm quantum cascade laser," *Applied Optics*, 2013, 52(19): 4613–4619.

[22] P. Geiser, "New opportunities in mid-infrared emission control," *Sensors* (*Basel*), 2015, 15(9): 22724–22736.

[23] J. Reid and D. Labrie, "2nd-harmonic detection with tunable diode-lasers-comparison of experiment and theory," *Applied Physics B–Photophysics and Laser Chemistry*, 1981, 26(3): 203–210.

[24] T. R. S. Hayden and G. B. Rieker, "Large amplitude wavelength modulation spectroscopy for sensitive measurements of broad absorbers," *Optics Express*, 2016, 24(24): 27910–27921.